

Protective effects of erythropoietin against cuprizone-induced oxidative stress and demyelination in the mouse corpus callosum

Iraj Ragerdi Kashani ^{1*}, Hossein Chavoshi ¹, Parichehr Pasbakhsh ¹, Mahmoud Hassani ², Ameneh Omid ³, Reza Mahmoudi ⁴, Cordian Beyer ⁵, Adib Zendedel ⁵

¹ Department of Anatomy, School of Medicine, Tehran University of Medical Sciences, Tehran, Iran

² Department of Medical Nanotechnologies, School of Advanced Technologies, Tehran University of Medical Sciences, Tehran, Iran

³ Department of Anatomical Sciences, Medical Sciences Faculty, Tarbiat Modares University, Tehran, Iran

⁴ Cellular and Molecular Research Center, Yasuj University of Medical Sciences, Yasuj, Iran

⁵ Faculty of Medicine, Institute of Neuroanatomy, RWth Aachen University, Aachen, Germany

ARTICLE INFO

Article type:

Original article

Article history:

Received: Oct 4, 2016

Accepted: Jan 12, 2017

Keywords:

Cuprizone

Demyelination

Erythropoietin

Multiple sclerosis

Oxidative stress

ABSTRACT

Objective(s): Increasing evidence in both experimental and clinical studies suggests that oxidative stress plays a major role in the pathogenesis of multiple sclerosis. The aim of the present work is to investigate the protective effects of erythropoietin against cuprizone-induced oxidative stress.

Materials and Methods: Adult male C57BL/6J mice were fed a chow containing 0.2 % cuprizone for 6 weeks. After 3 weeks, mice were simultaneously treated with erythropoietin (5,000 IU/ kg body weight) by daily intraperitoneal injections.

Results: Our results showed that cuprizone induced oxidative stress accompanied with down-regulation of subunits of the respiratory chain complex and demyelination of corpus callosum. Erythropoietin antagonized these effects. Biochemical analysis showed that oxidative stress induced by cuprizone was regulated by erythropoietin. Similarly, erythropoietin induced the expression of subunits of the respiratory chain complex over normal control values reflecting a mechanism to compensate cuprizone-mediated down-regulation of these genes.

Conclusion: The data implicate that erythropoietin abolishes destructive cuprizone effects in the corpus callosum by decreasing oxidative stress and restoring mitochondrial respiratory enzyme activity.

► Please cite this article as:

Ragerdi Kashani I, Chavoshi H, Pasbakhsh P, Hassani M, Omid A, Mahmoudi R, Beyer C, Zendedel A. Protective effects of erythropoietin against cuprizone-induced oxidative stress and demyelination in the mouse corpus callosum. Iran J Basic Med Sci 2017; 20:886-893. doi: 10.22038/IJBMS.2017.9110

Introduction

Multiple sclerosis (MS) is a demyelinating neurodegenerative disease in which both environmental and genetic factors appear to have a causal role (1). Although the pathogenesis of MS has not been fully defined, oligodendrocyte death with subsequent demyelination and tissue destruction play crucial roles in the pathophysiology of MS (2). According to a report published by Lucchinetti *et al.* (3), there are 4 different lesion subtypes in MS. Pattern 1 and 2 lesions may be mediated by autoimmunity, while both pattern 3 and 4 lesions were presumed to be a primary oligodendroglialopathy (4). Although the exact molecular function of each of these patterns can be varied, they share a common feature; that is, the tissue injury mechanisms are closely related to the production of reactive oxygen (5) and mitochondrial dysfunction (6). Mitochondrial dysfunction is caused by several factors. However, cellular energy crises and increased oxidative stress are the consequences of mitochondrial dysfunction (7). Oxidative stress is defined as an alteration in the delicate balance between prooxidant and antioxidant

enzymes in cells which cause severe oxidative damage and ultimately compromise cell viability (8). Since CNS is a high oxygen consumer, it is particularly sensitive to oxidative stress (9). It is likely that microglia is a major source of ROS in the MS (10). Erythropoietin also known as EPO is a glycoprotein hormone that controls erythropoiesis and is mainly secreted by interstitial fibroblasts in the adult kidney (11). In addition to the kidney, it has also been reported that EPO is secreted mostly by astrocytes in the central nervous system (12). Previous studies showed that EPO or EPO-derivatives are the protective factors that can modulate the immune responses by several biochemical pathways in experimental immune models of demyelination (13-16). It was shown that EPO, possibly through amelioration of inflammation-associated axonal degeneration in the white matter tracts, dampens neurological symptoms in a non-immune toxin model of MS (17). Based on pharmacological properties of EPO, in the present study, it was proposed that EPO might ameliorate demyelination by decreasing oxidative stress in a non-immune cuprizone model of MS.

*Corresponding author: Iraj Ragerdi Kashani. Department of Anatomical Sciences, School of Medicine, Tehran University of Medical Sciences, 16 Azar Street, Poursina Street, Tehran, Iran. Fax: +98-2166419072; email: ragerdi@tums.ac.ir

Materials and Methods

Animals

Research and animal care were approved by the Review Board for the Care of Animal Subjects of the District Government (Tehran, Iran). *In vivo* experiments were performed with 8 weeks old male C57BL/6 mice (approx. 20 g, Pasteur, Iran). Animals were housed under temperature-controlled conditions with alternate light and dark cycles, 12 hr each and *ad libitum* access to water and food.

Experimental design

Eight-week-old (20 g) male c57Bl/6 mice were randomly divided into three groups (n=10 per group). One group was fed normal diet and served as controls. The two other groups received diets containing 0.2% (w/w) cuprizone (Sigma-Aldrich, Germany) for a total of 6 weeks (Sigma, USA) to induce demyelination. After 3 weeks, mice were injected every other day (21 injections in total) with phosphate buffer saline (PBS) or erythropoietin (EPO) (5,000 IU/kg body weight intraperitoneally; Roche, Basel, Switzerland) up to the end of cuprizone feeding. The chosen EPO dose closely resembled that used in another study on treating the CPZ model of MS in mice (17). The three groups were as follows: control group which was fed normal diet (Cont), PBS-treated cuprizone group (CPZ), and erythropoietin-treated cuprizone group (CPZ+EPO). Mice were anesthetized with ketamine (115 mg/kg) (Sigma, USA) and xylazine (10 mg/kg) (Sigma, USA) and killed after 6 weeks. Animal handling and treatment protocols have been previously described in detail (18).

Luxol fast blue staining

Myelination was analyzed in sections by Luxol Fast Blue (LFB, Sigma, USA). Sections were placed overnight in LFB at 56 °C and washed in 95% ethanol and distilled water to remove the excess blue stain. The color was then differentiated (until the white matter was easily distinguishable from gray matter) in a lithium carbonate solution for 15 sec, followed by distilled water and three 80% alcohol washing steps. Slices were further passed through fresh xylene twice, mounted with Entellan (Merck, Germany) and covered. To evaluate demyelination in LFB stained sections, three independent blinded readers scored LFB stained sections between zero and three. To score the myelin status we assigned score 3 to the non-demyelinated and 0 to the totally demyelinated corpus callosum mice. A score of one or two corresponds to one-third or two-third fiber myelination of the corpus callosum, respectively.

Transmission electron microscopy

For electron microscopic examination, three animals per group were transcardially perfused with 2% glutaraldehyde and 2% paraformaldehyde in 0.1

M PBS. Brains were quickly removed and placed on ice. The corpus callosum was dissected, and the samples were placed in a tube. Samples were then placed, immediately after extraction, in 2.5% glutaraldehyde (Fluka) in 0.1 M cacodylate buffer (pH 7.4) at 4 °C overnight and transferred to 1% osmium tetroxide in the same buffer for 1 hr at room temperature. Tissue was transversely cut into 1 mm blocks which were further fixed in osmium tetroxide at 4 °C overnight, dehydrated through ascending ethanol washes, and embedded in epoxy resin (TAAB Laboratories). One- μ m sections were cut, stained with toluidine blue, and examined by light microscopy to identify demyelinated areas. Selected areas were subsequently examined by transmission electron microscopy (IEO 906 Germany, 100 kV). Sagittal sections of the corpus callosum were used for quantitative evaluation to determine the percentage of correctly myelinated axons per field according to the previous study (18). Corpus callosum images were taken from four sections. Photographs of axons orientated in cross-section were taken, and quantification of myelinated axons was performed on four images per animal and treated at a magnification of X3500 using the Image J software.

Immunohistochemistry (IHC)

Animals were anesthetized with 100 μ l of a ketamine: xylazine 3:1 mixture, sacrificed, and transcardially perfused with PBS followed by 4% paraformaldehyde (PFA, Sigma, Germany) in 0.1 M PBS, pH 7.4. Brains were removed, post-fixed in 4% PFA overnight and rinsed with PBS. After overnight post-fixation, brains were dissected, embedded, and then coronary processed into 5 μ m sections from the levels 215 to 275 according to the mouse brain atlas by Sidman *et al.* (<http://www.hms.harvard.edu/research/brain/atlas.html>). For IHC, sections were placed on silane-coated slides, deparaffinized, rehydrated, heat unmasked, and finally blocked with PBS containing 5% normal serum. Afterwards, sections were exposed overnight at 4 °C to the following primary antibodies: mouse anti-glia fibrillary acidic protein (GFAP) monoclonal antiserum (1:1,000, Serotec, Germany), mouse anti-olig2 (oligodendrocytes, 1:1,000, Abcam, UK) and mouse anti-Iba-1 (microglia 1:4000, Wako, Richmond, VA). The next day, sections were treated with H₂O₂/PBS (0.3%) (Roth, Germany) for blocking endogenous peroxidase. Then, sections were incubated with the appropriate secondary antibodies followed by the ABC complex. Diaminobenzidine (DAB) was used as a chromogen. Finally, sections were counterstained with hematoxylin, dehydrated in graded alcohols, and mounted. Quantification of oligodendrocytes, astrocytes, and microglia was performed by manually counting the number of positive olig2, GFAP, and Iba2 cells in the corpus callosum, respectively. For each animal, a total of four slices were analyzed with

a distance of 150 μm in between. Counting was performed using a Nikon Eclipse 55i (Nikon) and 20 \times and 40 \times objectives. Cell numbers are expressed as cells per mm^2 . All morphological quantification was performed in a blinded way where the reader was not aware of the treatment.

Biochemical analysis

In order to assess free radical-mediated effects following cuprizone-induced demyelination with or without EPO treatment, estimations of lipid peroxidation (LPO), reduced glutathione (GSH) and superoxide dismutase (SOD) tissue levels were carried out in the corpus callosum. To this end, mice were transcidentally perfused with 0.1 M PBS (Sigma, USA). Brains were then taken out, and the corpus callosum was dissected. Tissues were then homogenized on ice using a tissue homogenizer (Remi, India). LPO products (malondialdehyde; MDA) in the corpus callosum were measured according to Kashani *et al* (18). In brief, brain homogenates were prepared in 0.15 M KCl (5% w/v homogenate). Aliquots of 0.6 ml were incubated for 0 and 1 hr at 37 °C. Subsequently, 1.2 ml of 28% w/v trichloroacetic acid (TCA) solution (5%) was added, and the volume was made up to 3 ml by adding 1.2 ml of water. Following centrifugation at 3,000 g for 10 min, 2.5 ml of the supernatant was taken and the color was developed by addition of 0.5 ml of 1% w/v thiobarbituric acid dissolved in 0.05 N NaOH keeping the solution in boiling water bath for 15 min until the appearance of pink color. The absorbance was read at 532 nm in a spectrophotometer. MDA contents were expressed as nmol/g wet tissue. The GSH content of corpus callosum was also determined by spectrophotometer. Briefly, proteins from homogenized tissues (10% w/v in PBS, pH 7.4) were removed by adding an equal volume of 10% TCA allowing to stand at 4 °C for 2 hr. The samples were then centrifuged at 2000 g for 15 min, and the supernatant was added to 2 ml of 0.4 M Tris buffer (pH 8.9) containing 0.02 M EDTA (pH 8.9) (Sigma, USA) followed by the addition of 0.01 M 5, 5'-Dithio-bis 2-Nitrobenzoic acid. Finally, the mixture was diluted with 0.5 ml distilled water and absorbance was read in a spectrophotometer at 412 nm. Results are expressed as μg GSH/g wet tissue. Total SOD activity in the corpus callosum homogenate was measured based on the ability of SOD to inhibit the production of formazan dye resulted from the reaction of WST-1 (water-soluble tetrazolium salt) and superoxide anion. Briefly, the sample was mixed with WST-1 solution and enzyme solution (xanthine oxidase) and incubated at 37 °C for 30 min. Then the absorbance of the solution at 450 nm was measured. The activity of total SOD in the brain tissue was calculated by referring to the standard curve and expressed as U/mg protein.

Table 1. Primer list

Primer	Sequence	AT
Cox2		
S	AACCGAGTCGTTCTGCCAAT	60 °C
AS	AACCTGGTCGGTTTGATGTT	
Cytb		
S	ACGAAAAACACACCCATTATTT	61 °C
AS	CCGTTTGGGTGTATATATCGGATT	
Nd1		
S	TTTACGAGCCGTAGCCCAAA	58–60 °C
AS	GGCCGGCTCGGTATTCTAC	
Atp6		
S	AGCAGTCCGGTTACAGCTAA	63 °C
AS	GGAGGGTGAATACGTAGGCTTG	
Hprt		
S	GCTGGTGAAAAGGACCTCT	62 °C
AS	CACAGGACTAGAACACCTGC	

S: sense; A: antisense; AN: annealing temperature

Semi-quantitative reverse transcriptase polymerase chain reaction (sqRT-PCR)

To determine mRNA transcript levels of catalytic subunits of the respiratory chain, sqRT-PCR was performed. Total RNA was extracted using the high Pure RNA Isolation Kit (Roche, Germany), DNase treated, and tested for its integrity by agarose gel electrophoresis. Two micrograms of each RNA sample was used for cDNA synthesis in a 60 min reaction at 42 °C using MuLV reverse transcriptase (Fermentas, Lithuania) in the presence of random hexamers and RNase inhibitor. Table 1 lists the primer pairs used for amplification of the following gene candidates: *Nd1* (complex I, NADH-ubiquinone oxidoreductase), *Cytb* (complex III, ubiquinol cytochrome c oxidoreductase), *Cox2* (complex IV, cytochrome c oxidase), and *Atp6* (complex V, Atp synthase). Hypoxanthine-guanine phosphoribosyl transferase (*Hprt*) served as internal control and was amplified to normalize relative levels of cDNA in different samples.

Statistical analysis

Data were analyzed for normality using the Kolmogorov-Smirnov test. All data are given as means \pm SD. Statistical differences between various groups were analyzed by one-way analysis of variance (ANOVA) followed by Tukey's *post hoc* test using GraphPad Prism 5 (GraphPad Software Inc., USA).

Results

EPO effects on cuprizone-induced changes in brain myelin status

Standard LFB staining revealed a normal myelin structure in the control group (Figure 1A). The animals treated with cuprizone and PBS (CPZ group) exhibited a significant decrease in LFB staining, characterized by light areas indicative of myelin disorganization (Figure 1B). In the animals treated with cuprizone and EPO (CPZ+EPO group), LFB staining was significantly stronger than in the CPZ

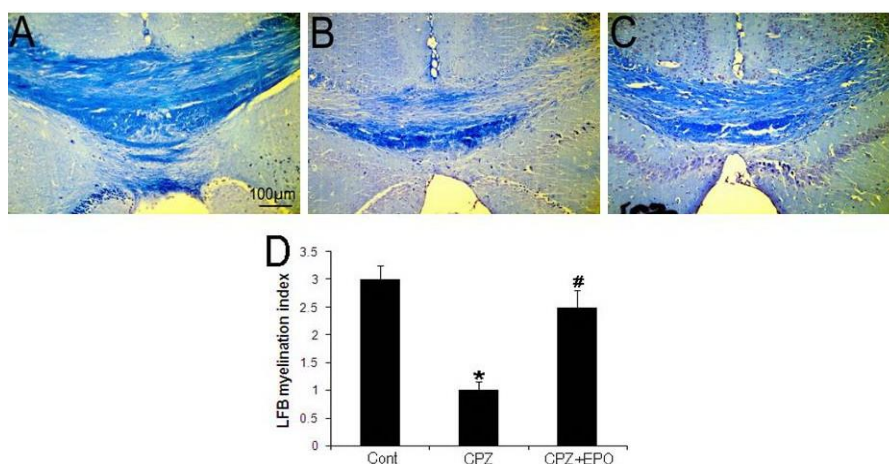


Figure 1. Demyelination in the corpus callosum after 6 weeks of cuprizone-induced demyelination concurrent treatment with phosphate buffer saline (CPZ group)(B), or erythropoietin (CPZ+EPO group)(C). Myelination index was evaluated in luxol fast blue (LFB) stained sections. The photomicrographs were taken from coronal sections of the corpus callosum. Quantification of the myelination index in the center of the corpus callosum reveals significant myelin loss in the cuprizone with phosphate buffer saline (CPZ) treatment compared with the control(Cont)(A, D) group and a restoration of myelin in the cuprizone with erythropoietin treatment group (CPZ+EPO)(C, D). Data represented mean ± SD. * $P \leq 0.05$ CPZ vs. Cont, # $P \leq 0.05$ CPZ vs. CPZ+EPO. Scale bar 100 μ m

group, but the myelin aspect was irregular and displayed vacuoles (Figure 1C). Semi-quantitative analysis of LFB-stained sections confirmed these observations (Figure 1D). Cuprizone significantly impaired the myelin score (1 ± 0.15 ; $P \leq 0.05$) when compared with controls (3 ± 0.26 ; $P \leq 0.05$). Applications of EPO, however, attenuated this negative effect (2.5 ± 0.3 ; $P \leq 0.05$).

Effect of EPO on Cuprizone-Induced Changes in the cellular composition of corpus callosum

Numbers of mature oligodendrocytes, astrocytes, and microglia were investigated by Olig2, GFAP, and Iba2 staining, respectively (Figure 2). In cuprizone group, corpus callosum contained reduced numbers

of olig2+ cells (216 ± 10 ; $P \leq 0.05$) compared to control (927 ± 21 ; $P \leq 0.05$) and this loss was significantly reversed in animals that received EPO (738 ± 29 ; $P \leq 0.05$) (Figures 2A, B, C, D). As shown in Figures 2E, F, G, and H, the cuprizone group showed increased GFAP+ cells compared to the control group. The number of GFAP+ cells increased from 59 ± 4 in the control group to 172 ± 6 ($P \leq 0.05$) in the cuprizone group and this increase was significantly reversed in animals that received EPO (84 ± 2 ; $P \leq 0.05$) (Figures 2G, H). The number of Iba2+ cells increased from 27 ± 1 in the control group to 86 ± 6 ($P \leq 0.05$) in the cuprizone group and this increase was significantly reversed in animals that received EPO (31 ± 1 ; $P \leq 0.05$) (Figures 2I, J, K, L).

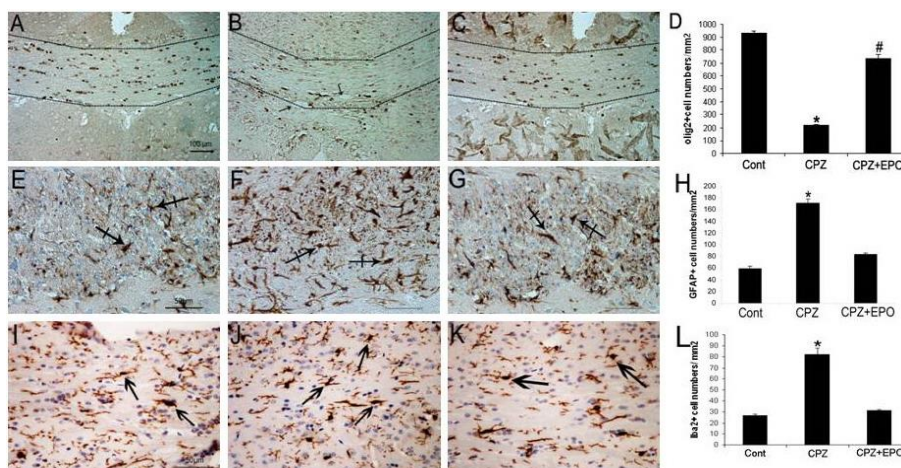


Figure 2. Effect of cuprizone-induced demyelination concurrent treatment with phosphate buffer saline (CPZ group) or erythropoietin (CPZ+EPO group) on the cellular composition of the corpus callosum(CC) demonstrated by anti-Olig2 (upper row), anti- GFAP (middle row) and anti-Iba2 (lower row) in the CC. In the CPZ group (Figure 2B), CC contained reduced numbers of olig2+ cells compared to the control (Cont) group (Figure 2A) and this loss was significantly reversed in animals that received EPO (Figures 2C, D). The number of GFAP+ cells (astrocytes) increased significantly in the CPZ group (Figure 2F) compared to the Cont group (Figure 2E) and this loss was significantly reversed in animals that received EPO (Figures 2G, H). In the CPZ group (Figure 2J), CC contained increased numbers of Iba2+ cells (microglia)(Figure 2J) compared to the control (Cont) group (Figure 2I) and this increase was significantly reversed in animals that received EPO (Figures 2K, L).). * $P \leq 0.05$ CPZ vs Cont, # $P \leq 0.05$ CPZ+EPO vs cuprizone. Scale bars, 100 μ m (A-C) and 50 μ m (E-G and I-K)

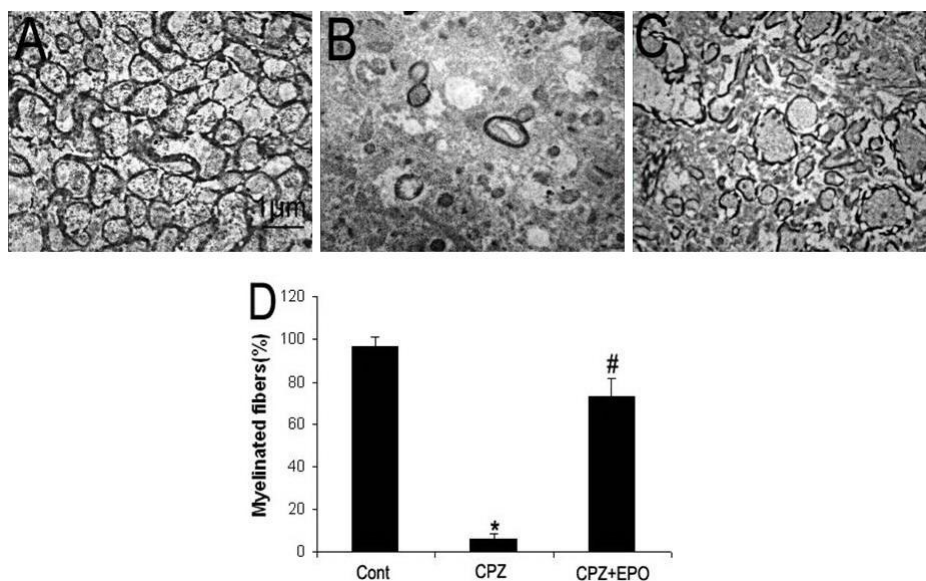


Figure 3. Representative transmission electron photographs of axons in the corpus callosum (CC) after 6 weeks of cuprizone-induced demyelination concurrent treatment with phosphate buffer saline (CPZ group)(B) or erythropoietin (CPZ+EPO group) (C). Micrographs show a massive decrease in the number of myelinated axons in the CC of CPZ group (B) compared with the Cont group (A) and a partial restoration of myelinated axon numbers in the CPZ+EPO group (C). Quantitative assessment confirmed this observation (D). Data represent mean \pm SD from three independent experiments, * $P \leq 0.05$ CPZ vs. Cont, # $P \leq 0.05$ CPZ vs. CPZ+EPO. Scale bar 1 μ m

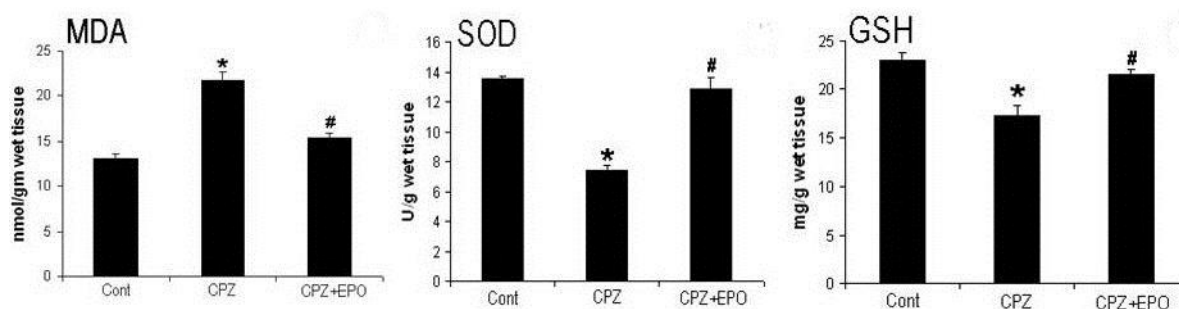


Figure 4. Effect of cuprizone-induced demyelination concurrent treatment with phosphate buffer saline (CPZ) or erythropoietin (CPZ+EPO) on the levels of malondialdehyde (MDA), superoxide dismutase (SOD), and reduced glutathione (GSH) in the corpus callosum. Cuprizone with PBS (CPZ) reduced SOD and GSH but increased MDA compared with the control (Cont) group. Cuprizone with EPO (CPZ+EPO) reversed the effect on SOD and GSH. EPO exposure itself lowered MDA levels compared with the control group. Data represented mean \pm SD. * $P \leq 0.05$ CPZ vs. Cont, # $P \leq 0.05$ CPZ+EPO vs

Effect of EPO on Cuprizone-Induced Changes in the myelination index of corpus callosum

The transmission electron microscopic photographs were used to determine the percentage of myelinated axons in the corpus callosum of control, cuprizone with or without EPO administration (Figure 3). We observed a decrease in the percentage of myelinated axons in the absence of EPO treatment compared to control group ($P < 0.05$; Figures 3A, B, D). Co-administration of EPO with cuprizone significantly increased this percentage to approximately 80% ($P \leq 0.05$; Figures 3C, D).

Effect of EPO on cuprizone-induced changes in the brain oxidative stress status

In order to analyze the effects of cuprizone and EPO exposure on distinctive parameters for oxidative

stress, we determined MDA, SOD, and GSH levels in homogenates of the corpus callosum. As shown in Figure 4A, MDA levels were significantly increased after cuprizone feeding ($P \leq 0.05$, 2B) compared with control mice. This effect was antagonized by the application of EPO. In contrast, GSH and SOD levels were significantly decreased after cuprizone feeding ($P = 0.1891$, 2B) compared with control mice. Interestingly, EPO exposure significantly ($P \leq 0.05$) increased GSH and SOD levels ($P \leq 0.05$) compared with cuprizone fed mice.

Effect of epo on cuprizone-induced changes in expression of mitochondrial respiratory chain genes

We have investigated the expression levels of distinct catalytic subunits of the four mitochondrial respiratory chain complexes *Atp6*, *Nd1*, *Cytb*, and

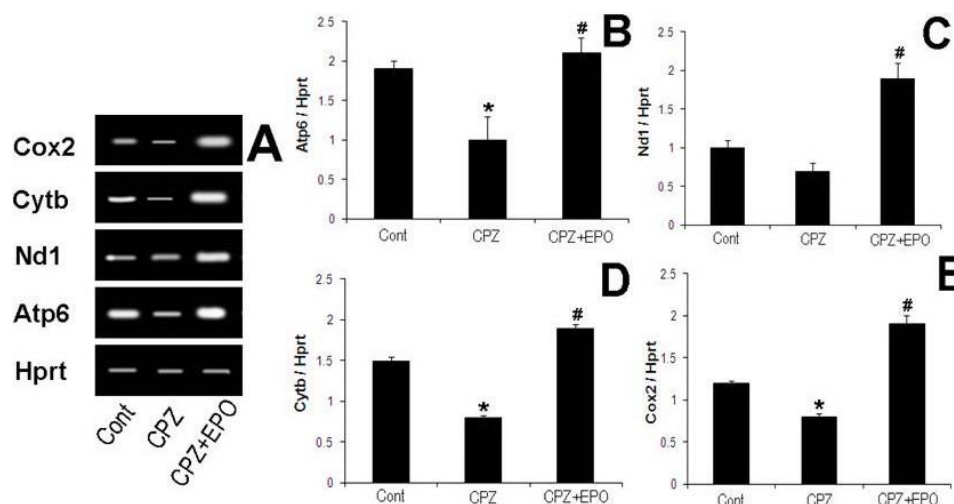


Figure 5. Semi-quantitative PCR analysis of corpus callosum tissues after cuprizone-induced demyelination concurrent treatment with phosphate buffer saline (CPZ) or erythropoietin (CPZ+EPO) on levels of subunits of the mitochondrial respiratory chain genes: Atp6 (A, B), Nd1 (A, C), Cytb (A, D), Cox2 (A, E). Hypoxanthine-guanine phosphoribosyl transferase (Hprt) was used as an internal control. Densitometry analysis of the bands normalized against Hprt is shown in the histograms. Data represent mean \pm SD from three independent experiments, * $P \leq 0.05$ CPZ vs. Cont, # $P \leq 0.05$ CPZ vs. CPZ+EPO

Cox2 by sqRT-PCR. Our data show that all four subunits are massively down-regulated after cuprizone exposure without EPO treatment and that the administration of EPO significantly increases levels of all four subunits well above levels of control animals ($P \leq 0.05$, cuprizone versus cuprizone + EPO, Figure 5).

Discussion

The ameliorative effects of EPO on cuprizone-induced demyelination have been demonstrated in this work. Clinical and laboratory data indicate that there is one important mechanism of tissue injury in all lesions at all stages of the MS, which is related to oxidative damage, mediated by activated macrophages and microglia (3, 19, 20). Oxidative injury leads to mitochondrial dysfunction, which is prominent in active MS lesions (21), and mitochondrial injury can explain many essential pathological features of MS lesions, such as oligodendrocyte apoptosis, demyelination, degeneration of thin caliber axons, and functional and structural disturbances of microglia, astrocytes, and oligodendrocyte progenitor cells (22). In this study, we used cuprizone, which can cause oxidative damage to oligodendrocytes and dystrophic axons in the corpus callosum and other white matter areas of the brain and has been found to closely resemble so-called pattern III lesions in MS patients (3, 18). It has been postulated that cuprizone is a copper chelating drug, which triggers apoptosis in oligodendrocytes and induces demyelination through mechanisms of oxidative injury (23). Cuprizone-induced demyelination is accompanied by the accumulation of microglia and astrocyte, similar to MS (24). Here, we showed that cuprizone diet significant-

ly increased MDA and decreased activities of the antioxidant enzymes such as SOD and GSH. These results are consistent with previous reports (18, 25). Cuprizone as a toxic model of demyelination was able to produce increased MDA, as a marker of free radical-mediated LPO, a simultaneous decrease of GSH levels and antioxidant enzyme activity (SOD)(4). Although extensive evidence implicates increased ROS production in demyelinating diseases, the underlying mechanisms of ROS-dependent myelin loss are not yet clarified (18). It is believed that ROS induced oligodendrocyte apoptosis directly and indirectly. Under *in vitro* conditions oligodendrocytes have been shown to be sensitive to ROS and NO concentrations in much lower concentrations than toxic concentrations of other glial cells, astrocytes, and microglia (26). Indirect effects of ROS on the apoptosis of oligodendrocytes were induced by glutamate (27). The excitotoxicity of glutamate is mediated through reduction of cysteine concentration, which leads to the reduction of GSH concentration,

too (20). In this study, we demonstrated that administration of EPO significantly inhibits MDA generation and prevents oxidative stress in terms of GSH decrease induced by cuprizone. The efficiency of EPO in maintaining the homeostasis of LPO and GSH was shown in several experimental models (28-30). Furthermore, the normalization of MDA levels by concurrent treatment with EPO might have resulted from the inhibitory effect of EPO on LPO (31). One possible mechanism responsible for the EPO-induced decrease in LPO may concern inhibition to iron-catalyzed free radical reactions (28). On the other hand Sims *et al.* (32) showed that glutathione levels are increased in the presence of EPO due to upregulation of the cysteine-glutamate exchanger,

system Xc^- , which is responsible for the cellular import of cysteine for the synthesis of glutathione. Although clear evidence is lacking including its ability to function as a direct scavenger but our results confirm the previous finding regarding the antioxidant action of EPO (29, 30). Another amplification factor of oxidative stress is the liberation of divalent iron from degenerating oligodendrocytes may be the reason for microglia activation, mitochondrial injury, and amplification of oxidative stress, have been suggested as a major driving force of demyelination and neurodegeneration in MS (33). In this study, we found a relationship between microglial accumulation and demyelination in our study. It demonstrates that accumulation and activation of microglia in the demyelinated lesion has harmful aspects on corpus callosum. Some of the mechanisms that are being proposed to explain these detrimental roles are: the recruitment and reactivation of T cells in the CNS through the release of proteases, the production of proinflammatory cytokines, and the release of reactive oxygen species to induce neurotoxicity and OPC toxicity through excitatory amino acids (34). We observed a massive down-regulation of Atp-6, Nd1, Cytb, and Cox2, as subunits of the respiratory chain complexes, after cuprizone exposure, which was antagonized by concurrent EPO administration. EPO has been shown to regulate mitochondrial homeostasis through the control of mitochondrial oxidative phosphorylation enzymes and the synthesis of ATP (35). Our observations are in line with these findings concerning the regulation of subunits of the respiratory chain enzyme complexes. Importantly, EPO not only restored the basal levels but further boosted the expression of complexes I-IV. This would allow compensating for any oxidative challenge of cells and improving the energy balance.

In conclusion, our data indicate that EPO can abolish destructive cuprizone effects in the corpus callosum by decreasing oxidative stress and increasing respiratory enzyme complex capacity. These findings may encourage the use of EPO, a compound established as clinically safe, in the treatment of human MS patients and are suited as therapeutic options.

Conclusion

The data indicate that EPO abolishes destructive cuprizone effects in the corpus callosum by decreasing oxidative stress and restoring mitochondrial respiratory enzyme activity.

Acknowledgment

The results presented in this study were part of a student thesis, which was financially supported by Tehran University of Medical Sciences, Tehran, Iran (grant no: 93-02-30-25746).

References

- Xia Z, White CC, Owen EK, Von Korff A, Clarkson SR, McCabe CA, et al. Genes and Environment in Multiple Sclerosis project: A platform to investigate multiple sclerosis risk. *Ann Neurol* 2016; 79:178-189.
- Vakilzadeh G, Khodagholi F, Ghadiri T, Darvishi M, Ghaemi A, Noorbakhsh F, et al. Protective effect of a cAMP analogue on behavioral deficits and neuropathological changes in cuprizone model of demyelination. *Mol Neurobiol* 2015; 52:130-141.
- Lucchinetti C, Brück W, Parisi J, Scheithauer B, Rodriguez M, Lassmann H. Heterogeneity of multiple sclerosis lesions: implications for the pathogenesis of demyelination. *Ann Neurol* 2000; 47:707-717.
- Praet J, Guglielmetti C, Berneman Z, Van der Linden A, Ponsaerts P. Cellular and molecular neuropathology of the cuprizone mouse model: clinical relevance for multiple sclerosis. *Neurosci Biobehav Rev* 2014; 47:485-505.
- Haidar L. Inflammation, iron, energy failure, and oxidative stress in the pathogenesis of multiple sclerosis. *Oxid Med Cell Longev* 2015; 2015:725370.
- Dadhania VP, Trivedi PP, Vikram A, Tripathi DN. Nutraceuticals against Neurodegeneration: A Mechanistic Insight. *Curr Neuropharmacol* 2016; 14:627-640.
- Kasote DM, Hegde MV, Katyare SS. Mitochondrial dysfunction in psychiatric and neurological diseases: cause(s), consequence(s), and implications of antioxidant therapy. *Biofactors* 2013; 39:392-406.
- Sinha K, Das J, Pal PB, Sil PC. Oxidative stress: the mitochondria dependent and mitochondria-independent pathways of apoptosis. *Arch Toxicol* 2013; 87:1157-1180.
- Carvalho AN, Lim JL, Nijland PG, Witte ME, Van Horsen J. Glutathione in multiple sclerosis: more than just an antioxidant? *Mult Scler* 2014; 20:1425-1431.
- Liu J, Tian D, Murugan M, Eyo UB, Dreyfus CF, Wang W, et al. Microglial Hv1 proton channel promotes cuprizone-induced demyelination through oxidative damage. *J Neurochem* 2015; 135:347-356.
- Kaneko N, Kako E, Sawamoto K. Enhancement of ventricular-subventricular zone-derived neurogenesis and oligodendrogenesis by erythropoietin and its derivatives. *Front Cell Neurosci* 2013; 7:235.
- Csete M, Rodriguez L, Wilcox M, Chadalavada S. Erythropoietin receptor is expressed on adult rat dopaminergic neurons and erythropoietin is neurotrophic in cultured dopaminergic neuroblasts. *Neurosci Lett* 2004; 359:124-126.
- Yuan R, Maeda Y, Li W, Lu W, Cook S, Dowling P. Erythropoietin: a potent inducer of peripheral immunoinflammatory modulation in autoimmune EAE. *PLoS One* 2008; 3:e1924.
- Najmi Varzaneh F, Najmi Varzaneh F, Azimi AR, Rezaei N, Sahraian MA. Efficacy of combination therapy with erythropoietin and methylprednisolone in clinical recovery of severe relapse in multiple sclerosis. *Acta Neurol Belg* 2014; 114:273-278.
- Cervellini I, Ghezzi P, Mengozzi M. Therapeutic efficacy of erythropoietin in experimental autoimmune encephalomyelitis in mice, a model of multiple sclerosis. *Methods Mol Biol* 2013; 982:163-173.
- Cervellini I, Annenkov A, Brenton T, Chernajovsky Y, Ghezzi P, Mengozzi M. Erythropoietin (EPO) increases myelin gene expression in CG4 oligodendrocyte cells through the classical EPO receptor. *Mol Med* 2013; 19:223-229.

17. Hagemeyer N, Boretius S, Ott C, Von Streitberg A, Welpinghus H, Sperling S, *et al.* Erythropoietin attenuates neurological and histological consequences of toxic demyelination in mice. *Mol Med* 2012; 18:628-635.
18. Kashani IR, Rajabi Z, Akbari M, Hassanzadeh G, Mohseni A, Eramsadati MK, *et al.* Protective effects of melatonin against mitochondrial injury in a mouse model of multiple sclerosis. *Exp Brain Res* 2014; 232:2835-2846.
19. Suneetha A, Raja Rajeswari K. Role of dimethyl fumarate in oxidative stress of multiple sclerosis: A review. *J Chromatogr B Analyt Technol Biomed Life Sci* 2016; S1570-0232:30090-30093.
20. Lassmann H. What drives disease in multiple sclerosis: Inflammation or neurodegeneration? *Clin Exp Neuroimmunol* 2010; 1:2-11.
21. Lassmann H. Pathology and disease mechanisms in different stages of multiple sclerosis. *J Neurol Sci* 2013; 333:1-4.
22. Torkildsen Ø, Brunborg LA, Thorsen F, Mørk SJ, Stangel M, Myhr KM, *et al.* Effects of dietary intervention on MRI activity, de- and remyelination in the cuprizone model for demyelination. *Exp Neurol* 2009; 215:160-166.
23. Lassmann H, Bradl M. Multiple sclerosis: experimental models and reality. *Acta Neuropathol* 2016; [Epub ahead of print] Review.
24. Tanaka T, Murakami K, Bando Y, Yoshida S. Minocycline reduces remyelination by suppressing ciliary neurotrophic factor expression after cuprizone induced demyelination. *J Neurochem* 2013; 127:259-270.
25. Acs P, Kipp M, Norkute A, Johann S, Clarner T, Braul A, *et al.* 17beta estradiol and progesterone prevent cuprizone provoked demyelination of corpus callosum in male mice. *Glia* 2009; 57:807-814.
26. Ljubisavljevic S, Stojanovic I. Neuroinflammation and demyelination from the point of nitrosative stress as a new target for neuroprotection. *Rev Neurosci* 2015; 26: 49-73.
27. Kostic M, Zivkovic N, Stojanovic I. Multiple sclerosis and glutamate excitotoxicity. *Rev Neurosci* 2013; 24:71-88.
28. Akisu M, Tuzun S, Arslanoglu S, Yalaz M, Kultursay N. Effect of recombinant human erythropoietin administration on lipid peroxidation and antioxidant enzyme(s) activities in preterm infants. *Acta Med Okayama* 2001; 55:357-362.
29. Bailey DM, Lundby C, Berg RM, Taudorf S, Rahmouni H, Gutowski M, *et al.* On the antioxidant properties of erythropoietin and its association with the oxidative-nitrosative stress response to hypoxia in humans. *Acta Physiol (Oxf)* 2014; 212:175-187.
30. Yildirim E, Ozisik K, Solaroglu I, Kaptanoglu E, Beskonakli E, Sargon MF, *et al.* Protective effect of erythropoietin on type II pneumocyte cells after traumatic brain injury in rats. *J Trauma* 2005; 58:1252-1258.
31. Akdemir Ozisik P, Oruckaptan H, Ozdemir Geyik P, Misirlioglu M, Sargon MF, Kilinc K, *et al.* Effect of erythropoietin on brain tissue after experimental head trauma in rats. *Surg Neurol* 2007; 68:547-555.
32. Sims B, Clarke M, Njah W, Hopkins ES, Sontheimer H. Erythropoietin induced neuroprotection requires cysteine glutamate exchanger activity. *Brain Res* 2010; 1321:88-95.
33. Hametner S, Wimmer I, Haider L, Pfeifenbring S, Brück W, Lassmann H. Iron and neurodegeneration in the multiple sclerosis brain. *Ann Neurol* 2013; 74:848-861.
34. Rawji KS, Yong VW. The benefits and detriments of macrophages/microglia in models of multiplesclerosis. *Clin Dev Immunol* 2013; 2013:948976.
35. Plenge U, Belhage B, Guadalupe-Grau A, Andersen PR, Lundby C, Dela F, *et al.* Erythropoietin treatment enhances muscle mitochondrial capacity in humans. *Front Physiol* 2012; 3:50.